Published in final edited form as:
Eur Neuropsychopharmacol. 2009 September ; 19(9): 670–681. doi:10.1016/j.euroneuro.2009.03.007.

Modulation of the Ca^{2+} Conductance of Nicotinic Acetylcholine Receptors by Lypd6

Martin Darvas[1,‡], **Marco Morsch**[2,‡], **Ildiko Racz**[1], **Seifollah Ahmadi**[2], **Dieter Swandulla**[2], and **Andreas Zimmer**[1]

[1]Institute of Molecular Psychiatry, University of Bonn, Bonn, Germany

[2]Institute of Physiology, University of Bonn, Bonn, Germany

Abstract

The agonist binding sensitivity and desensitization kinetics of nicotinic acetylcholine receptors (nAChRs) can be modulated by snake venom neurotoxins and related endogenous small proteins of the uPAR-Ly6 family. Here we identify Lypd6, a distantly related member of the u-PAR/Ly-6 family expressed in neurons as a novel modulator of nAChRs. Lypd6 overexpressed in trigeminal ganglia neurons selectively enhanced the Ca2+-component of nicotine-evoked currents through nAChRs, as evidenced by comparative whole-cell patch clamp recordings and Ca2+-imaging in wildtype and transgenic mice overexpressing Lypd6. In contrast, a knockdown of Lypd6 expression using siRNAs selectively reduced nicotine-evoked Ca2+-currents. Pharmacological experiments revealed that the nAChRs involved in this process are heteromers. Transgenic mice displayed behaviors that were indicative of an enhanced cholinergic tone, such as a higher locomotor arousal, increased prepulse-inhibition and hypoalgesia. These mice overexpressing Lypd6 mice were also more sensitive to the analgesic effects of nicotine. Transgenic mice expressing siRNAs directed against Lypd6 were unable to procreate, thus indicating a vital role for this protein. Taken together, Lypd6 seems to constitute a novel modulator of nAChRs that affects receptor function by selectively increasing Ca2+-influx through this ion channels.

Keywords

transgenic mice; allosteric modulator; Ion selectivity; electrophysiology; behavior; receptor channel

Introduction

Nicotinic acetylcholine receptors (nAChRs) belong to the “Cys-loop superfamily” of ligand-gated ion channels that are gated by the neurotransmitter acetylcholine, as well as nicotine, the major psychoactive component in tobacco. They have an important role in various functions of the central nervous system (CNS) including memory, locomotion, sensorimotor gating and pain sensation (Dani, 2001, Everitt and Robbins, 1997, Picciotto et al., 2000, Tassonyi et al., 2002). Based upon their expression and subunit composition, nAChRs can have quite different

Correspondence: Andreas Zimmer, Institute of Molecular Psychiatry, University of Bonn, Sigmund-Freud Str. 25, D-53127 Bonn, Germany. E-mail: E-mail: neuro@uni-bonn.de; Phone:+49 228 / 688 5300; Fax +49 228 / 688 5301.
‡The first two authors contributed equally to this work

effects on neurotransmission. Presynaptic and preterminal nAChRs enhance neurotransmitter release (Lena et al., 1993, McGehee et al., 1995), postsynaptic nAChRs convey fast excitatory transmission (Hefft et al., 1999, Roerig et al., 1997) and nonsynaptic nAChRs have effects on many neurotransmitter systems by modulating neuronal excitability (Descarries et al., 1997, Vizi, 2000). In these processes influx of Ca^{2+} through nAChR-channels plays an important functional role (Dani, 2001, Vizi, 2000).

Nicotinic acetylcholine receptors represent a prototype of allosteric proteins. In addition to modulation through allosteric effectors such as divalent cations, natural steroid hormones (Curtis et al., 2002), drugs like 5-hydroxyindole (Zwart et al., 2002), PNU-120596 (Hurst et al., 2005) or ivermectin (Krause et al., 1998), several endogenous small proteins with homology to alpha-neurotoxins have been identified that bind nAChRs and modulate their activity (Hogg et al., 2005).

On neurons, the GPI-anchored protein Lynx1 alters current amplitudes and desensitization kinetics of α4/β2-nAChRs (Ibanez-Tallon et al., 2002, Miwa et al., 1999). Genetic deletion of Lynx1 in mice resulted in an increased sensitivity of nAChRs to nicotine and a prolonged nAChR receptor activation (Miwa et al., 2006). In the epidermis, the secreted proteins Slurp1 and Slurp2 regulate keratinocyte nAChRs (Adermann et al., 1999, Arredondo et al., 2006, Arredondo et al., 2005). Mutations in the human SLURP1 gene cause Mal de Meleda, an autosomal recessive inflammatory and palmoplantar skin disorder (Chimienti et al., 2003). Lynx1, Slurp1 and Slurp2 belong to the murine u-PAR/Ly-6 gene family, which is evolutionary related to the elapid snake venom neurotoxins (Fleming et al., 1993, Gumley et al., 1995). Most other members of the u-PAR/Ly-6 gene family code for GPI-linked cell accessory proteins of the immune system (Gumley et al., 1995, Hanninen et al., 1997, Mallya et al., 2006).

In this study we report the identification of a novel member of the u-PAR/Ly6 gene family, Lypd6 (LY6/PLAUR domain containing 6 (Ploug and Ellis, 1994)), which modulates nicotinic receptor signaling in vivo. Sequence analysis of Lypd6 and other members of the snake venom neurotoxin superfamily support a direct evolutionary relationship between Lypd6 and well-known endogenous modulators of cholinergic transmission like Lynx1, Slurp1 and Slurp2. Lypd6 is highly expressed in the brain and spinal cord. Lypd6-deficient and overexpressing transgenic mice reveal that Lypd6 acts as a modulator of nAChRs and is also essential for embryo development.

Materials and methods

Generation of siRNA knockdown transgenic mice

To generate Lypd6 RNAi-inducing small hairpin RNA, we cloned 21 bp of the mouse Lypd6 coding region (5'– GGGAACAGCAUCUCUGUCAUU -3') into the pLL3.7 vector (Rubinson et al., 2003) as an inverted repeat with a 9-bp spacer. The pLL3.7 vector contains a U6 promoter and a floxed, CMV promoter driven EGFP reporter gene. Six FVB/N transgenic founders were bred with FVB/N wild-type mice.

Generation of synapsin-Lypd6 transgenic mice

The Lypd6 ORF was fused to the amino-terminus of the HA epitope (YPYDVPDYA). The expression construct used the rat synapsin1 promoter (Dittgen et al., 2004) and a bovine growth hormone polyA-signal. Transgenic FVB/N founders were bred with FVB/N wild-type mice. Three different lines, D17, D67 and D774 were analyzed. D17 and D67 expressed the transgene, while D774 did not. The data presented in the main manuscript text are mostly derived from the D17 founder, using D774 as a non-expressing control.

Transgene DNA analysis

Genomic DNA from tail biopsies was analyzed by Southern blot with Digoxigenin-(Dig) labeled EGFP (siRNA transgenes) or Lypd6 (Synapsin-Lypd6 transgenes) probes. Diglabeled probes were generated by PCR amplification with Dig-dNTPs (Boehringer-Mannheim) using the following primers: EGFP probe forward: 5'- GCC ACA AGT TCA GCG TGT C-3', EGFP probe reverse: 5'- CTG CTT GTC GGC CAT GAT A -3', Lypd6 Probe forward: 5'- ATC TGC ACC TCC TGC TGT GAA -3' and Lypd6 Probe reverse: 5'- TTA TAA GGT GAG TCC CAG CCA -3'.

Quantitative RT-PCR

Tissues were dissected from 8 – 12 week old wild-type or transgenic mice and frozen immediately. RNA was extracted with TRIzol reagent (Invitrogen), digested with DNase I (Roche), and purified using the RNeasy Kit (QIAGEN). The analysis was performed independently with five animals. Five μg RNA was reverse-transcribed (Superscript II, Invitrogen). Parallel samples without reverse transcriptase served as controls for non-specific DNA amplification. TATA binding protein (TBP) primers were used as internal control and Lypd6 primers were used to amplify a region of the endogenous Lypd6 transcript (TBP forward: 5'-AAA GAC CAT TGC ACT TCG TGC-3'; TBP reverse: 5'-AAA TCA ACG CAG TTG TCC GTG-3', Lypd6 forward: 5'-CCT GAC ATC TAC TGT CCT CG-3'; Lypd6 reverse: 5'-CTT GTA GCC TTC GTG CTC-3'). PCR reactions (40 cycles) and detections were carried out with the SYBR® Green JumpStart™ system (Sigma Aldrich) in an Opticon DNA Engine (MJ Research). Expression levels were calculated with the $2^{-\Delta\Delta CT}$ method (Livak and Schmittgen, 2001), using dorsal root ganglion expression as calibrator. RT-PCR analysis for the expression analysis of 2310010M24Rik mRNA was performed with the following primers: 2310010M24Rik forward: 5'-TGT TTC AGT CCA AAG ACG CCT-3' and 2310010M24Rik reverse: 5'-TAG AAT GTG GCA GAG GAG CA-3'. RT-PCR analysis for the expression analysis of Lypd6-HA mRNA was performed with the following primers: Lypd6 forward: 5'-CCT GAC ATC TAC TGT CCT CG-3' and HA reverse: 5'- TTA AGC GTA ATC AGG TAC GTC GTA AGG GTA-3′.

In-situ hybridization

In situ hybridization was performed on 12 μm sections of fresh frozen adult (8–12 weeks) mouse brain with sense and antisense riboprobes. Digoxigenin- (Dig-) labeled sense and antisense riboprobes (150 bp) were transcribed from Lypd6 (position 357 – 597; NM_177139) using 0.5 μM Dig-UTP (Boehringer-Mannheim).

Western blot analysis

Brain and testis protein extracts were immunoprecipitated with an anti-HA mouse monoclonal antibody (clone 16B12; Covance), incubated with protein G, thoroughly washed and suspended in sample buffer. The immunoprecipitates were run on 12.5% SDS-PAGE and immuno-stained with anti-HA rabbit polyclonal antibody (1:500; Abcam), goat anti-rabbit horseradish peroxidase antibody (1:10,000; Jackson ImmunoResearch) and enhanced chemiluminescence (Pierce).

Transfection experiments

Mouse Neuro-2a cells (ATCC CCL-131) were plated at 70–90% confluency without antibiotics. Cells were transfected with empty vector (pLL3.7), a plasmid expressing small hairpin siRNA against LacZ-mRNA (psiRNA-LacZ) or pLL3.7-Lypd6. Cells were harvested 36 h after transfection and RNA was isolated and processed as described.

Behavioral tests

Mice were housed 3 – 6 per cage with a 12 h light/dark cycle (on 7:00 a.m.; off 7:00 p.m.). Food and water were available *ad libitum*. Behavioral tests were only performed during the light period except for home cage activity. Animal procedures were approved by the Bezirksregierung Köln. The observer was always blind to genotype. Independent animals were used for all behavioral tests.

Locomotor activity was assessed by the open field test for 60 minutes (Bilkei-Gorzo et al., 2008). Results were analyzed in 5 min intervals by an automated system equipped with infrared beams (TSE Systems). Home cage activity of single-housed mice was determined for 72 h with sampling periods of 5 minutes. Recognition memory was measured in the Y-maze. Each arm was 30 cm long, 8 cm wide and 16 cm high. Animals were placed at the cross-section of the maze and allowed to visit the arms freely for 5 min. Total number of arm entries and the number of arm alternations was recorded. Anxiety was measured in an elevated O-maze with a diameter of 53 cm (Bilkei-Gorzo et al., 2008). Mice were placed in the closed part of the maze and allowed free access for 10 min. A video tracking system (TSE Systems) was used to calculate the number of entries into the open and closed areas. To measureme the acoustic startle reaction, mice were placed in a startle chamber (TSE Systems) and exposed to 60 db background noise for 5 minutes, followed by 10 trials with 20 ms noise bursts (80 db, 100 db or 110 db). The inter-trial time was varied randomly between 20 – 40 s. The PPI test included 5 initial startle stimuli (110 dB of 20 ms duration) followed by 10 trials with 20 ms noise bursts (110 db) and 20 ms noise bursts (110 db) preceded by 20 ms prepulse bursts (80 db) 100 ms before the noise bursts. The presentation of trials followed a random pattern. The percent PPI was calculated as a percentage score: %PPI = 100 – ([(startle response to noise burst with prepulse burst trial)/(startle response to noise burst alone trial)] x 100) and averaged over the 10 trials. Antinociceptive responses were measured using a tail-flick apparatus (Columbus Instruments) (Bilkei-Gorzo et al., 2004). A cut-off latency of 10 s was used to prevent tissue damage. Measurements were made before and 3 min after acute subcutaneous nicotine (0.125, 0.25, 0.35 0.5, 0.625, 0.75 or 1 mg/kg) or saline administration. Nicotine was dissolved in saline and administered in a volume of 0.1 ml per 10 g of body weight. Data were expressed as percentage of maximum possible effect: (MPE %) = [(test latency – control latency) / (cut-off time - control latency)] x 100. Antinociception was also assessed by the writhing test (Racz et al., 2005). Three min prior to the injection of 0.6% acetic acid (0.1 ml per 10 g body weight), animals received an intraperitoneal injection (on the contra lateral site) of nicotine (0.25, 0.5 or 1 mg/kg, free base, 0.05 ml per 10 g body weight) or saline. Writhes were assessed for the next 30 min.

Preparation of trigeminal ganglia for electrophysiological recordings

Trigeminal ganglion neurons (TrigGs) were isolated from postnatal day 21 – 40. Animals were anesthetized with ether, decapitated, the brains removed and the heads transferred to ice-cold artificial cerebrospinal fluid (ACSF). Ganglia were isolated and digested ~20 minutes at 33° C. Enzymatic treatment w as stopped and tissues were triturated. The resulting suspension was filtered and centrifuged. The pelleted cells were resuspended and plated on poly-L-lysine coated (0.01 %) cover slips. Cells were maintained at 36°C in an incubator (5 % CO_2) and used for electrophysiological recordings within the next 20 hours.

Electrophysiological recordings

Coverslips were transferred to a recording chamber and constantly superperfused at 2 ml/min with normal external solution MMR (NaCl 145 mM, KCl 2.5 mM, $MgCl_2$ 1.3 mM, $CaCl_2$ 2 mM, Glucose 20 mM, HEPES 10 mM, pH 7.35) at room temperature. TrigGs were visualized using an Axiovert 200 inverted microscope (Zeiss). Patch pipettes (resistance 2–4 MΩ) filled with normal internal solution (KCl 130 mM, NaCl 10 mM, $MgCl_2$ 5 mM, EGTA 10 mM,

HEPES 10 mM, pH 7.35) were used for whole-cell recordings (Axopatch 200A amplifier, Axon Instruments; interface ITC-18, Instrutech Corp). The data were analyzed with Pulse (HEKA Elektronik). Membrane currents were sampled at 5 kHz. Solutions for isolation of calcium current components through nAChR channels were: Extracellular solution (in mM): Cholinechlorid 120, TEA-hydroxid 20, $CaCl_2$ 2, $MgCl_2$ 1, 4-Amino-Pyridine (4-AP) 4, Glucose 10, HEPES 10, pH 7.35. Intracellular solution (in mM): CsCl 140 or cholinechloride 140, MgCl 1, Mg-ATP 2, Na-GTP 0.05, BAPTA 10, HEPES 10, pH 7.35. Chemicals were purchased from Sigma-Aldrich. A pressure application system DAD-VC (ALA Scientific Instruments) was used for rapid application of drugs to TrigGs. Nicotine (Nic), mecamylamine (MEC), α-bungarotoxin (α-Btx) and methyllycaconitine (MLA) were purchased from Sigma-Aldrich. The tip of the application pipette (100 μm inner diameter) was placed ~50 μm away from the cell under investigation. In some experiments cells were incubated with α-Btx (100 nM) for about 10 – 30 minutes before nicotine application. very 'n' represents a different cell (animals used for each study were ≥ 5).

Microfluorometric calcium measurements

TrigG-cells were incubated at 37°C with the membran e-permanent fluorescent dye fura-2-AM (5 μM) for 60 min in DMEM:F12. Intracellular calcium transients were measured using an imaging system from TILL-Photonics. Changes in intracellular Ca^{2+}-concentration were expressed as ΔF/F, the ratio-time resolved fluorescence variations over the basal fluorescence. Extracellular solutions were (in mM): NaCl 145; KCl 2.5; $MgCl_2$ 1.3; $CaCl_2$ 10; Glucose 20; HEPES 10; pH 7.35. 100 μM $CdCl_2$ was added.

For knock-down studies cells were incubated 24 hours with 50 nM siRNA against Lypd6 (Stealth 770, 5'GCC ACA UUU GCU ACC ACA UCA CCU A3'; 5'UAG GUG AUG UGG UAG CAA AUG UGG C3'; Invitrogen) in DMEM. This siRNA reduced expression by more than 90 % in a CHO cell line expressing Lypd6 under a CMV promoter. Control experiments were performed in untreated cells, cells treated with siRNA against Firefly Luciferase (50 nM) and cells treated only with HiPerFect transfection medium (Qiagen). After incubation (24 hours) cells were prepared for microfluorometric measurements.

Data analysis and statistics

All data are presented as means ± SEM. Pair wise comparison of means was carried out with the Mann-Whitney test. Multiple comparisons were made with two-way ANOVA, followed by *post hoc* Bonferroni's test. $P < 0.05$ was considered significant.

Results

Identification of Lypd6 as a member of the uPAR/Ly-6 gene family

We have recently screened the mouse transcriptome for secreted small proteins with a putative neuromodulatory function using a computational approach (Gustincich et al., 2003, Okazaki et al., 2002). This led to the identification of 90 novel hypothetical neuromodulators, of which we now selected 39 candidates that had (i) a predicted open reading frame of 100 – 200 amino acids, (ii) a gene structure with intron-exon boundaries and (iii) additional support from ESTs. When we established expression profiles of these candidates, we found that one, Lypd6, (Figure 1A) displayed a prominent expression in the central nervous system (CNS) and in peripheral neurons, but only weakly in non-neuronal tissues (Figure 2). The short (516 bp) open reading frame of Lypd6 encodes a protein with a predicted size of 19 kDa (Figure 1B). Sequence comparison using the ClustalW algorithm (http://www.ebi.ac.uk/clustalw/) revealed a weak homology to a u-PAR/Ly-6 domain that is characterized by a conserved pattern of 8 – 10 cysteine residues and a C-terminal asparagine residue (Figure 1C; (Behrendt et al., 1991)). Most of the members of the murine u-PAR/Ly-6 gene family originated from local gene

duplication events and map to chromosome 15 (Hogarth et al., 1987), while Lypd6 is located on chromosome 2 (Okazaki et al., 2002). Interestingly, there is also another closely related transcript immediately upstream to Lypd6 (2310010M24Rik), implying that a common precursor of these genes became separated from the original segment of the u-PAR/Ly-6 gene cluster. Indeed, phylogenetic analysis showed that Lypd6 is most closely related to 2310010M24Rik (55% homology), followed by Lynx1 and SLURP1 (Figure 1D). The phylogenetic conservation suggested to us that these proteins may also share some common functions, thus offering the intriguing possibility that Lypd6 is a novel modulator of nAChRs.

Expression of Lypd6 in the mouse CNS

Reverse transcription real-time PCR analysis demonstrated that Lypd6 mRNA is highly enriched in brain and spinal cord, as well as dorsal root and trigeminal ganglia (Figure 2A). In situ hybridization to adult brain sections showed that Lypd6 is expressed in the deeper layers of the cerebral cortex (Figure 2B) and multiple other brain structures, including the nucleus of the vertical limb of the diagonal band of Broca (Figure 2C), the central medial, intermediodorsal, centrolateral and paraventricular thalamic nuclei (Figure 2D) and the dorsomedial hypothalamic nuclei (Figure 2E). We also found a low level of expression in some non-neuronal tissues including ovary, testes, spleen, skeletal muscle and kidney by RT-PCR (Figure 2A).

Generation of Lypd6-deficient mice

To study the function of Lypd6 we first blocked transcription by transgene expression of a small hairpin siRNA directed against the Lypd6 transcript. In cell culture, the construct reduced Lypd6 mRNA expression by 70% (Figure 3). A total of six transgenic founders were generated using pronucleus injection into oocytes (3 males, 3 females; Table 1). The first male died within 8 weeks after birth, probably as a result of a large abdominal cyst. The second male was successfully mated, but produced almost no transgenic offspring. Only two offspring (out of 82) were transgenic and these were unable to procreate. The third male produced only a single litter with three pups, none of which were transgenic. We sacrificed four females that were successfully plugged by this male at E10.5, but found no implantation sites. The three female founders could be mated, but they had also small litter sizes (2 – 3 pups per litter) with no transgene expression. It thus appears that the Lypd6 knockdown resulted in an impaired germ cell and/or embryonic development.

Mice with neuronal overexpression of Lypd6

We therefore produced next transgenic mice with a neuronal overexpression of Lypd6 (Figure 4A). The transgene was strongly expressed in brain, spinal cord, trigeminal and dorsal root ganglia (Figure 4B). The Lypd6 overexpressing animals showed no gross abnormalities in size, viability or CNS morphology (data not shown). In order to determine if Lypd6 affects nicotinic receptor function, we next evaluated behaviors that are modulated by cholinergic neurotransmission and/or nicotine administration (Champtiaux and Changeux, 2004, Dani, 2001, Marubio et al., 1999, Maskos et al., 2005, Picciotto et al., 2000, Picciotto et al., 1995, Stevens and Wear, 1997). Transgenic mice showed initially a much higher locomotor activity in the open field than wild-type controls, but quickly habituated to the environment and were similarly active as wild type controls after 60 minutes (Figure 5A). In contrast to that, transgenic mice showed fewer rearings in the open field (Figure 5B), thus indicating that the increased activity is not due to an increased exploratory drive. When we monitored the activity over 3 days in the home cage, we found that the transgenic animals were not more active when they were tested in an environment that was more familiar to them than the open field arena (Figure 5C). We also found an increased activity of transgenic animals in the 0-maze test. Nevertheless, the ratio of open arm to closed arm entries was similar in wild-type and transgenics, thus anxiety

levels were probably not affected. In the Y-maze test, transgenic mice were again significantly more active. The increased activity was not only significant for new arm entries (correct choice), but also for the total number of arm entries (Figure 5D). Therefore the ratio of correct choices was higher in transgenic mice compared to wild-type animals, indicating an improved working memory.

Both genotypes showed similar baseline startle responses to acoustic stimuli (Figure 5E), but transgenic mice showed a significantly higher prepulse inhibition (PPI) (Figure 5F), demonstrating enhanced sensorimotor gating in transgenic animals (Geyer et al., 2002). Thermal nociceptive responses in the tail-flick test were similar in transgenic and wild-type mice. However, transgenic animals showed fewer visceral pain responses in the acetic acid-induced writhing test. Nicotine administration produced a dose-dependent analgesia in both tests and genotypes. In transgenic animals, however, the nicotine dose-response curve was shifted significantly to the left (Transgenics ED_{50} = 0.4573 (0.4186 – 0.4996) mg/kg; Wild type ED_{50} = 0.5874 (0.5768 – 0.5983) mg/kg) in the tail-flick test (Figure 5G). In the writhing test, a nicotine dose of 0.25 mg/kg was already maximally effective in transgenic animals, while wild-type animals showed a dose-dependent increase in nicotine analgesia, with doses up to 1 mg/kg (Figure 5H).

Electrophysiological recordings in Lypd6 overexpressing mice

To further elucidate a possible role of Lypd6 in nicotine sensitivity of mice overexpressing Lypd6 we recorded currents through nAChR-channels in trigeminal ganglion neurons (TrigGs) of wild-type and transgenic mice using the whole-cell configuration of the patch clamp technique. We choose TrigGs because of the strong co-expression of nAChRs and Lypd6 in these neurons. Cells with diameters ≥ 18 μm (Genzen et al., 2001) were used in our experiments. Total currents through nAChR-channels did not differ significantly in peak amplitude and kinetics in wild-type compared to transgenic mice (Figure 6AB). The characteristics of the corresponding dose-response curves were comparable (Figure 6C). Nicotine concentrations needed to induce currents through nAChR-channels were rather high compared to those described in the literature (Fucile et al., 2005). Indeed, in control experiments we found that in wistar rats and C57BL/6 mice nicotine concentrations up to 100 μM were sufficient to induce substantial current responses to nicotine application. From this we conclude that the high nicotine concentrations needed in the present experiments are due to specific receptor properties of this mouse line. In subsequent experiments we isolated sodium, potassium and calcium components of the total currents through nAChR-channels. For the sodium and potassium current components, no significant difference in peak amplitudes and kinetics could be found between the two genotypes. However, peak amplitudes of the calcium current component, which accounted for a small fraction of the total current peak amplitudes (10 – 20 %), were significantly larger in transgenic mice in comparison to wild-type mice (Figure 6B). The characteristics of the dose response curves for total receptor currents did not differ significantly between wild-type and transgenic mice (Figure 6C).

Total currents as well as calcium currents were reversibly blocked (approximately 80 %) by the nAChR antagonist mecamylamine (MEC, 10 and 20 μM), but were unaffected by alpha-bungarotoxin (α-Btx, 10 and 100 nM) and methyllycaconitine (MLA, 20 nM) (Figure 7), indicating a specific involvement of non-α7-nAChRs in these responses. Our results suggest that Lypd6 specifically affects the calcium currents through nAChR-channels.

Microfluorometric calcium measurements

We further investigated the effect of Lypd6 on Ca2+ conductance by performing microfluorometric measurements of calcium transients in TrigGs. Changes in intracellular calcium concentration were measured in cells loaded with Fura-2-AM after blockade of

voltage-activated Ca^{2+}-channels by adding $CdCl_2$ (100 μM) to the external solution. In TrigGs of transgenic mice calcium transients evoked by nicotine (1 and 3 mM) were significantly larger in comparison to wild-type animals ($p < 0.0001$, data not shown).

We next inactivated Lypd6 using specific siRNA (Stealth 770), which suppressed endogenous Lypd6 expression by more than 90 % in TrigGs. Microfluorometric calcium measurements of these cells revealed a significant reduction of nicotine-induced intracellular calcium transients after siRNA treatment, compared to untreated cells from wild-type mice and compared to cells treated with a off-target or control siRNAs (Figure 8). Thus, transgenic overexpression of Lypd6 increased calcium currents through nAChR-channels, while a knockdown of the endogenous Lypd6 reduced nicotine-induced Ca^{2+} transients.

Discussion

The experiments we have presented in this paper identify Lypd6 as a member of the uPAR/Ly-6 gene family that is highly enriched in the CNS and acts as a novel modulator of nAChRs in mice. As a consequence of this peak amplitudes of nicotine-induced calcium currents through nAChR-channels are significantly enhanced in trigeminal ganglial neurons (TrigGs) of Lypd6 overexpressing animals and much reduced in neurons with a siRNAinduced knock-down of Lypd6 expression.

Lypd6 contains a signaling peptide and a consensus sequence for a GPI anchor. It is therefore likely that Lypd6 is a secreted, membrane bound peptide, similar to Lynx1 (Ibanez-Tallon et al., 2004). Our results suggested that Lypd6 either enhances the Ca^{2+} permeability or alternatively the activity of nicotinic receptors in TrigGs. To address this question we blocked homomeric α7 receptors, which have the highest Ca^{2+} permeability of all nicotinic receptors (Fucile et al., 2005), with α-bungarotoxin and methyllycaconitine. This blockade did not affect the modulation of nicotine-induced currents by Lypd6, excluding α7 homomers as target for the modulatory action of Lypd6. It is therefore more likely that Lypd6 selectively enhances the Ca^{2+} permeability of αβ-heteromers. Further experiments are necessary, however, to address the exact subunit composition of nAChR involved in these processes.

Transgenic mice with neuronal overexpression of Lypd6 showed a marked increase in locomotor activity in the open field. Because transgenic mice also showed fewer rearings, it is likely that the initially higher activity resulted from an increased response to novelty (Grailhe et al., 1999) and was not caused by a generalized hyperactivity or an increased exploratory drive. This discovery is supported by the finding that overexpression of Lypd6 did not result in an increased activity when the animals were tested in an environment that was familiar to them or after a period of habituation. Moreover, analysis of the activity of the transgenic animals in the Y-maze and the O-maze confirmed the increased novelty responses found in the open field arena. Transgenic animals showed an enhanced prepulse inhibition and displayed a pronounced visceral hypoalgesia in tests of chemical-visceral nociception. Taken together, the increased novelty responses, enhanced sensorimotor gating and hypoalgesia in transgenic mice is consistent with a heightened nicotinergic tone (Abreu-Villaca et al., 2006, Decker et al., 1995, Decker et al., 2004, Geyer et al., 2002, Suto et al., 2001, Vincler and Eisenach, 2005). Indeed, our behavioral pharmacological studies demonstrated an increased sensitivity to nicotine in Lypd6 overexpressing animals.

Interestingly, there are several similarities between the Lypd6-overexpression and the Lynx1 knockout phenotypes (Miwa et al., 2006). Both mouse lines show an increased sensitivity to nicotine, as revealed by behavioral pharmacology and single cell recordings. They also have behavioral phenotypes that are consistent with an enhanced nicotinergic tone, like an enhanced PPI and visceral hypoalgesia in Lypd6 transgenics. These data suggest that Lynx1 and Lypd6

have opposite modulatory effects, with Lynx1 reducing and Lypd6 enhancing nAChR signaling. These peptides are co-expressed in the deep layers of the neocortex, in the spinal cord, and in dorsal root ganglia (Miwa et al., 1999; http://expression.gnf.org). Thus, both peptides may interact and modulate nAChRs to finetune neuronal activity. The importance of this modulatory system is exemplified by the observation that Lynx1 deficient mice suffer from a progressive neuronal degeneration and that the Lypd6 knockdown seems to be incompatible with embryo survival. It should be noted in this context that Lypd6 is also expressed in non-neuronal tissues such as spleen, skeletal muscle, kidney, ovary and testis. This non-neuronal expression may point to an additional role of Lypd6 and contribute to the knockdown phenotype. Nevertheless, allosteric modulation of nAChRs through Lypd6 is an important component of cholinergic signaling both in the CNS and the periphery. Thus it may provide a new target for drug discovery that could be used for the treatment of neurological disorders, such as Alzheimer's disease, by means of enhancing the neuronal cholinergic tone (Maelicke et al., 2001).

References

Abreu-Villaca Y, Queiroz-Gomes Fdo E, Dal Monte AP, Filgueiras CC, Manhaes AC. Individual differences in novelty-seeking behavior but not in anxiety response to a new environment can predict nicotine consumption in adolescent C57BL/6 mice. Behav Brain Res 2006;167:175–182. [PubMed: 16214235]

Adermann K, Wattler F, Wattler S, Heine G, Meyer M, Forssmann WG, Nehls M. Structural and phylogenetic characterization of human SLURP-1, the first secreted mammalian member of the Ly-6/uPAR protein superfamily. Protein Sci 1999;8:810–819. [PubMed: 10211827]

Arredondo J, Chernyavsky AI, Jolkovsky DL, Webber RJ, Grando SA. SLURP-2: A novel cholinergic signaling peptide in human mucocutaneous epithelium. J Cell Physiol 2006;208:238–245. [PubMed: 16575903]

Arredondo J, Chernyavsky AI, Webber RJ, Grando SA. Biological effects of SLURP-1 on human keratinocytes. J Invest Dermatol 2005;125:1236–1241. [PubMed: 16354194]

Behrendt N, Ploug M, Patthy L, Houen G, Blasi F, Dano K. The ligand-binding domain of the cell surface receptor for urokinase-type plasminogen activator. J Biol Chem 1991;266:7842–7847. [PubMed: 1850423]

Bilkei-Gorzo A, Racz I, Michel K, Darvas M, Maldonado R, Zimmer A. A Common Genetic Predisposition to Stress Sensitivity and Stress-Induced Nicotine Craving. Biol Psychiatry 2008;63:164–171. [PubMed: 17570348]

Bilkei-Gorzo A, Racz I, Michel K, Zimmer A, Klingmuller D, Zimmer A. Behavioral phenotype of pre-proenkephalin-deficient mice on diverse congenic backgrounds. Psychopharmacology (Berl) 2004;176:343–352. [PubMed: 15197532]

Champtiaux N, Changeux JP. Knockout and knockin mice to investigate the role of nicotinic receptors in the central nervous system. Prog Brain Res 2004;145:235–251. [PubMed: 14650919]

Chimienti F, Hogg RC, Plantard L, Lehmann C, Brakch N, Fischer J, Huber M, Bertrand D, Hohl D. Identification of SLURP-1 as an epidermal neuromodulator explains the clinical phenotype of Mal de Meleda. Hum Mol Genet 2003;12:3017–3024. [PubMed: 14506129]

Curtis L, Buisson B, Bertrand S, Bertrand D. Potentiation of human alpha4beta2 neuronal nicotinic acetylcholine receptor by estradiol. Mol Pharmacol 2002;61:127–135. [PubMed: 11752213]

Dani JA. Overview of nicotinic receptors and their roles in the central nervous system. Biol Psychiatry 2001;49:166–174. [PubMed: 11230867]

Decker MW, Anderson DJ, Brioni JD, Donnelly-Roberts DL, Kang CH, O′Neill AB, Piattoni-Kaplan M, Swanson S, Sullivan JP. Erysodine, a competitive antagonist at neuronal nicotinic acetylcholine receptors. Eur J Pharmacol 1995;280:79–89. [PubMed: 7498257]

Decker MW, Rueter LE, Bitner RS. Nicotinic acetylcholine receptor agonists: a potential new class of analgesics. Curr Top Med Chem 2004;4:369–384. [PubMed: 14754452]

Descarries L, Gisiger V, Steriade M. Diffuse transmission by acetylcholine in the CNS. Prog Neurobiol 1997;53:603–625. [PubMed: 9421837]

Dittgen T, Nimmerjahn A, Komai S, Licznerski P, Waters J, Margrie TW, Helmchen F, Denk W, Brecht M, Osten P. Lentivirus-based genetic manipulations of cortical neurons and their optical and electrophysiological monitoring in vivo. Proc Natl Acad Sci U S A 2004;101:18206–18211. [PubMed: 15608064]

Everitt BJ, Robbins TW. Central cholinergic systems and cognition. Annu Rev Psychol 1997;48:649–684. [PubMed: 9046571]

Fleming TJ, O'Huigin C, Malek TR. Characterization of two novel Ly-6 genes. Protein sequence and potential structural similarity to alpha-bungarotoxin and other neurotoxins. J Immunol 1993;150:5379–5390. [PubMed: 8515066]

Fucile S, Sucapane A, Eusebi F. Ca2+ permeability of nicotinic acetylcholine receptors from rat dorsal root ganglion neurones. J Physiol 2005;565:219–228. [PubMed: 15760934]

Genzen JR, van Cleve W, McGehee DS. Dorsal root ganglion neurons express multiple nicotinic acetylcholine receptor subtypes. J Neurophysiol 2001;86:1773–1782. [PubMed: 11600638]

Geyer MA, Mcilwain KL, Paylor R. Mouse genetic models for prepulse inhibition: an early review. Mol Psychiatry 2002;7:1039–1053. [PubMed: 12476318]

Grailhe R, Waeber C, Dulawa SC, Hornung JP, Zhuang X, Brunner D, Geyer MA, Hen R. Increased exploratory activity and altered response to LSD in mice lacking the 5-HT(5A) receptor. Neuron 1999;22:581–591. [PubMed: 10197537]

Gumley TP, Mckenzie IF, Sandrin MS. Tissue expression, structure and function of the murine Ly-6 family of molecules. Immunol Cell Biol 1995;73:277–296. [PubMed: 7493764]

Gustincich S, Batalov S, Beisel KW, Bono H, Carninci P, Fletcher CF, Grimmond S, Hirokawa N, Jarvis ED, Jegla T, Kawasawa Y, Lemieux J, Miki H, Raviola E, Teasdale RD, Tominaga N, Yagi K, Zimmer A, Hayashizaki Y, Okazaki Y. Analysis of the mouse transcriptome for genes involved in the function of the nervous system. Genome Res 2003;13:1395–1401. [PubMed: 12819138]

Hanninen A, Jaakkola I, Salmi M, Simell O, Jalkanen S. Ly-6C regulates endothelial adhesion and homing of CD8(+) T cells by activating integrindependent adhesion pathways. Proc Natl Acad Sci U S A 1997;94:6898–6903. [PubMed: 9192663]

Hefft S, Hulo S, Bertrand D, Muller D. Synaptic transmission at nicotinic acetylcholine receptors in rat hippocampal organotypic cultures and slices. J Physiol 1999;515(Pt 3):769–776. [PubMed: 10066903]

Hogarth PM, Mckenzie IF, Sutton VR, Curnow KM, Lee BK, Eicher EM. Mapping of the mouse Ly-6, Xp-14, and Gdc-1 loci to chromosome 15. Immunogenetics 1987;25:21–27. [PubMed: 2880797]

Hogg RC, Buisson B, Bertrand D. Allosteric modulation of ligand-gated ion channels. Biochem Pharmacol 2005;70:1267–1276. [PubMed: 16043127]

Hurst RS, Hajos M, Raggenbass M, Wall TM, Higdon NR, Lawson JA, Rutherford-Root KL, Berkenpas MB, Hoffmann WE, Piotrowski DW, Groppi VE, Allaman G, Ogier R, Bertrand S, Bertrand D, Arneric SP. A novel positive allosteric modulator of the alpha7 neuronal nicotinic acetylcholine receptor: in vitro and in vivo characterization. J Neurosci 2005;25:4396–4405. [PubMed: 15858066]

Ibanez-Tallon I, Miwa JM, Wang HL, Adams NC, Crabtree GW, Sine SM, Heintz N. Novel modulation of neuronal nicotinic acetylcholine receptors by association with the endogenous prototoxin lynx1. Neuron 2002;33:893–903. [PubMed: 11906696]

Ibanez-Tallon I, Wen H, Miwa JM, Xing J, Tekinay AB, Ono F, Brehm P, Heintz N. Tethering naturally occurring peptide toxins for cell-autonomous modulation of ion channels and receptors in vivo. Neuron 2004;43:305–311. [PubMed: 15294139]

Krause RM, Buisson B, Bertrand S, Corringer PJ, Galzi JL, Changeux JP, Bertrand D. Ivermectin: a positive allosteric effector of the alpha7 neuronal nicotinic acetylcholine receptor. Mol Pharmacol 1998;53:283–294. [PubMed: 9463487]

Lena C, Changeux JP, Mulle C. Evidence for “preterminal” nicotinic receptors on GABAergic axons in the rat interpeduncular nucleus. J Neurosci 1993;13:2680–2688. [PubMed: 8501532]

Livak KJ, Schmittgen TD. Analysis of relative gene expression data using real-time quantitative PCR and the 2(-Delta Delta C(T)) Method. Methods 2001;25:402–408. [PubMed: 11846609]

Maelicke A, Samochocki M, Jostock R, Fehrenbacher A, Ludwig J, Albuquerque EX, Zerlin M. Allosteric sensitization of nicotinic receptors by galantamine, a new treatment strategy for Alzheimer's disease. Biol Psychiatry 2001;49:279–288. [PubMed: 11230879]

Mallya M, Campbell RD, Aguado B. Characterization of the five novel Ly-6 superfamily members encoded in the MHC, and detection of cells expressing their potential ligands. Protein Sci 2006;15:2244–2256. [PubMed: 17008713]

Marubio LM, del Mar Arroyo-Jimenez M, Cordero-Erausquin M, Lena C, Le Novere N, de Kerchove D'Exaerde A, Huchet M, Damaj MI, Changeux JP. Reduced antinociception in mice lacking neuronal nicotinic receptor subunits. Nature 1999;398:805–810. [PubMed: 10235262]

Maskos U, Molles BE, Pons S, Besson M, Guiard BP, Guilloux JP, Evrard A, Cazala P, Cormier A, Mameli-Engvall M, Dufour N, Cloez-Tayarani I, Bemelmans AP, Mallet J, Gardier AM, David V, Faure P, Granon S, Changeux JP. Nicotine reinforcement and cognition restored by targeted expression of nicotinic receptors. Nature 2005;436:103–107. [PubMed: 16001069]

McGehee DS, Heath MJ, Gelber S, Devay P, Role LW. Nicotine enhancement of fast excitatory synaptic transmission in CNS by presynaptic receptors. Science 1995;269:1692–1696. [PubMed: 7569895]

Miwa JM, Ibanez-Tallon I, Crabtree GW, Sanchez R, Sali A, Role LW, Heintz N. lynx1, an endogenous toxin-like modulator of nicotinic acetylcholine receptors in the mammalian CNS. Neuron 1999;23:105–114. [PubMed: 10402197]

Miwa JM, Stevens TR, King SL, Caldarone BJ, Ibanez-Tallon I, Xiao C, Fitzsimonds RM, Pavlides C, Lester HA, Picciotto MR, Heintz N. The prototoxin lynx1 acts on nicotinic acetylcholine receptors to balance neuronal activity and survival in vivo. Neuron 2006;51:587–600. [PubMed: 16950157]

Okazaki Y, Furuno M, Kasukawa T, Adachi J, Bono H, Kondo S, Nikaido I, Osato N, Saito R, Suzuki H, Yamanaka I, Kiyosawa H, Yagi K, Tomaru Y, Hasegawa Y, Nogami A, Schonbach C, Gojobori T, Baldarelli R, Hill DP, Bult C, Hume DA, Quackenbush J, Schriml LM, Kanapin A, Matsuda H, Batalov S, Beisel KW, Blake JA, Bradt D, Brusic V, Chothia C, Corbani LE, Cousins S, Dalla E, Dragani TA, Fletcher CF, Forrest A, Frazer KS, Gaasterland T, Gariboldi M, Gissi C, Godzik A, Gough J, Grimmond S, Gustincich S, Hirokawa N, Jackson IJ, Jarvis ED, Kanai A, Kawaji H, Kawasawa Y, Kedzierski RM, King BL, Konagaya A, Kurochkin IV, Lee Y, Lenhard B, Lyons PA, Maglott DR, Maltais L, Marchionni L, Mckenzie L, Miki H, Nagashima T, Numata K, Okido T, Pavan WJ, Pertea G, Pesole G, Petrovsky N, Pillai R, Pontius JU, Qi D, Ramachandran S, Ravasi T, Reed JC, Reed DJ, Reid J, Ring BZ, Ringwald M, Sandelin A, Schneider C, Semple CA, Setou M, Shimada K, Sultana R, Takenaka Y, Taylor MS, Teasdale RD, Tomita M, Verardo R, Wagner L, Wahlestedt C, Wang Y, Watanabe Y, Wells C, Wilming LG, Wynshaw-Boris A, Yanagisawa M, et al. Analysis of the mouse transcriptome based on functional annotation of 60,770 full-length cDNAs. Nature 2002;420:563–573. [PubMed: 12466851]

Picciotto MR, Caldarone BJ, King SL, Zachariou V. Nicotinic receptors in the brain. Links between molecular biology and behavior. Neuropsychopharmacology 2000;22:451–465. [PubMed: 10731620]

Picciotto MR, Zoli M, Lena C, Bessis A, Lallemand Y, Le Novere N, Vincent P, Pich EM, Brulet P, Changeux JP. Abnormal avoidance learning in mice lacking functional high-affinity nicotine receptor in the brain. Nature 1995;374:65–67. [PubMed: 7870173]

Ploug M, Ellis V. Structure-function relationships in the receptor for urokinasetype plasminogen activator. Comparison to other members of the Ly-6 family and snake venom alpha-neurotoxins. FEBS Lett 1994;349:163–168. [PubMed: 8050560]

Racz I, Schutz B, Abo-Salem OM, Zimmer A. Visceral, inflammatory and neuropathic pain in glycine receptor alpha 3-deficient mice. Neuroreport 2005;16:2025–2028. [PubMed: 16317347]

Roerig B, Nelson DA, Katz LC. Fast synaptic signaling by nicotinic acetylcholine and serotonin 5-HT3 receptors in developing visual cortex. J Neurosci 1997;17:8353–8362. [PubMed: 9334409]

Rubinson DA, Dillon CP, Kwiatkowski AV, Sievers C, Yang L, Kopinja J, Rooney DL, Ihrig MM, Mcmanus MT, Gertler FB, Scott ML, van Parijs L. A lentivirus-based system to functionally silence genes in primary mammalian cells, stem cells and transgenic mice by RNA interference. Nat Genet 2003;33:401–406. [PubMed: 12590264]

Stevens KE, Wear KD. Normalizing effects of nicotine and a novel nicotinic agonist on hippocampal auditory gating in two animal models. Pharmacol Biochem Behav 1997;57:869–874. [PubMed: 9259018]

Suto N, Austin JD, Vezina P. Locomotor response to novelty predicts a rat's propensity to self-administer nicotine. Psychopharmacology (Berl) 2001;158:175–180. [PubMed: 11702091]

Tassonyi E, Charpantier E, Muller D, Dumont L, Bertrand D. The role of nicotinic acetylcholine receptors in the mechanisms of anesthesia. Brain Res Bull 2002;57:133–150. [PubMed: 11849819]

Vincler MA, Eisenach JC. Knock down of the alpha 5 nicotinic acetylcholine receptor in spinal nerve-ligated rats alleviates mechanical allodynia. Pharmacol Biochem Behav 2005;80:135–143. [PubMed: 15652389]

Vizi ES. Role of high-affinity receptors and membrane transporters in nonsynaptic communication and drug action in the central nervous system. Pharmacol Rev 2000;52:63–89. [PubMed: 10699155]

Zwart R, de Filippi G, Broad LM, Mcphie GI, Pearson KH, Baldwinson T, Sher E. 5-Hydroxyindole potentiates human alpha 7 nicotinic receptor-mediated responses and enhances acetylcholine-induced glutamate release in cerebellar slices. Neuropharmacology 2002;43:374–384. [PubMed: 12243767]

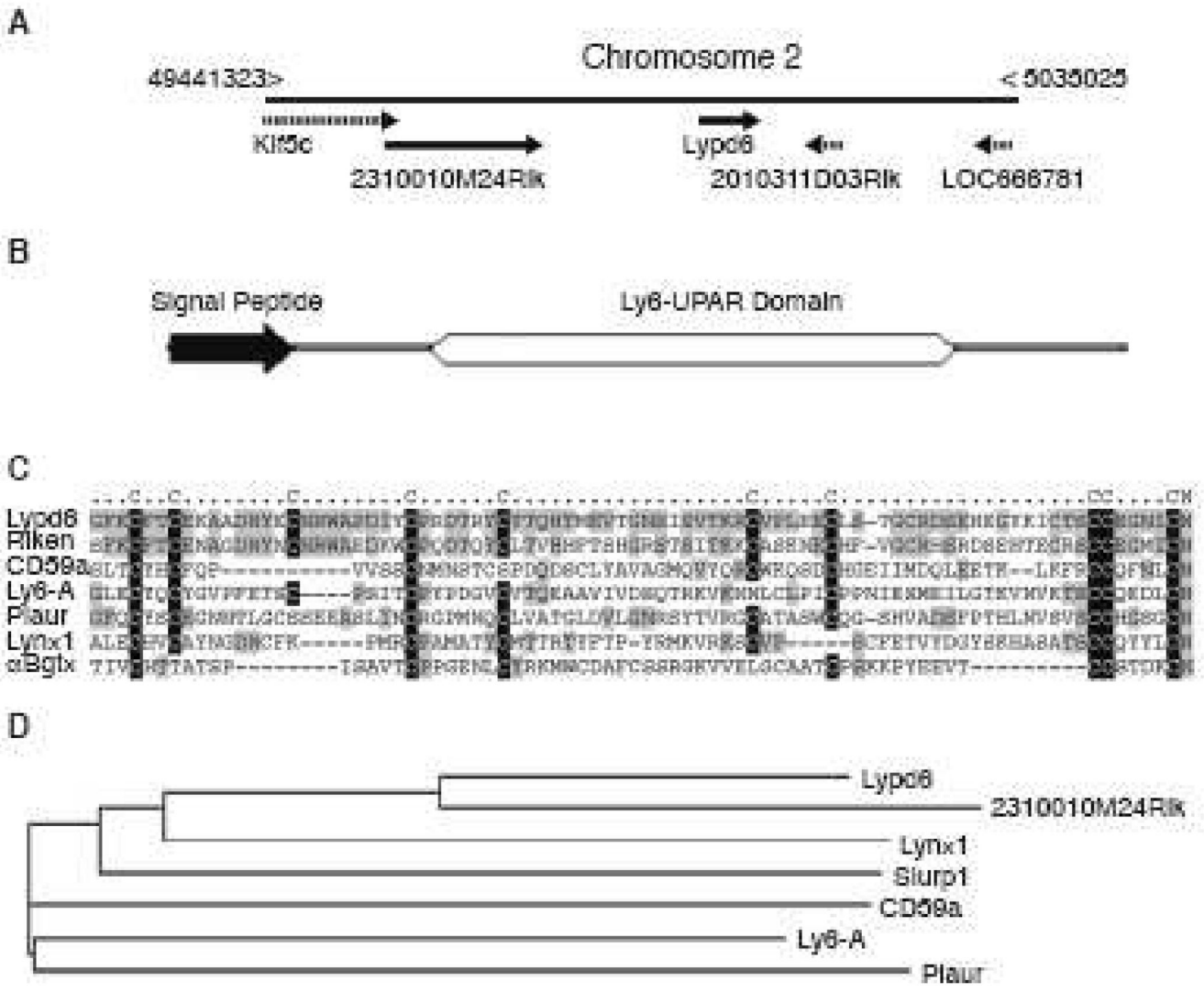

Figure 1. Structure and homology analysis of the murine Lypd6 protein

(A) The Lypd6 gene locus on chromosome 2 and the relative position of Lypd6 to its paralog gene 2310010M24Rik and other local genes. Direction of arrows indicates position on the (+)-strand (→) or the (−)-strand (←).

(B) Predicted protein features of the Lypd6 ORF. The black arrow demarcates the N-terminal consensus signal sequence (amino acids 1 – 22). The white box shows the u-PAR/Ly-6 domain (amino acids 47 – 141).

(C) Amino acid sequence homology between Lypd6, 2310010M24Rik (Riken) and other u-PAR/Ly-6 domain containing proteins of the Ly6/αBtx superfamily. These proteins comprise four groups: the lymphocyte cell surface antigens CD59a and Ly6-A, the urokinase-type plasminogen activator receptor Plaur, elapid snake venom neurotoxins αBgtx and the endogenous modulators of nAChRs Lynx1 and Slurp1. Only the sequence encoding the Ly6-UPAR domain was used for these alignments. The u-PAR/Ly-6 domain consensus motif is shown above. Residues corresponding to this motif are shaded in black. Residues matching the Lypd6 sequence are shaded in gray.

(D) Phylogenetic analysis of Lypd6 and other mouse u-PAR/Ly-6 domain proteins using the ClustalW algorithm with u-PAR/Ly-6 domain amino acid sequences.

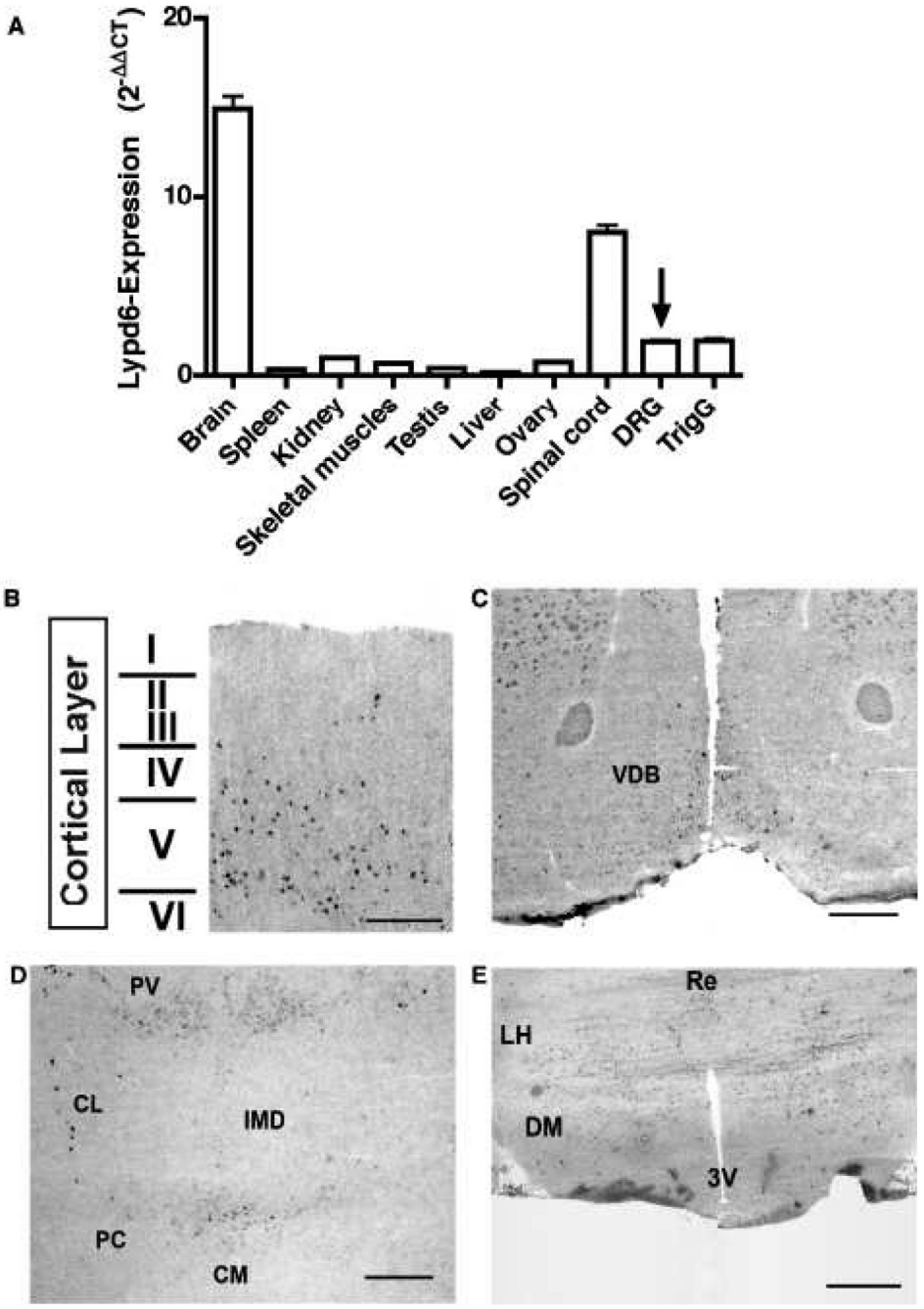

Figure 2. Expression of Lypd6 mRNA

(A) Quantitative analysis of Lypd6 expression in adult murine tissues by real-time PCR. Lypd6 expression was calculated as $\Delta\Delta C_T$ value: first the expression was normalized by TATA binding protein mRNA expression and then calibrated as fold change of the expression in dorsal root ganglia (indicated by an arrow). The analysis was performed independently with tissues from five animals. DRG = Dorsal root ganglia; TrigG = Trigeminal ganglia. Values are expressed as mean ± SEM.

(B - E) *In-situ* hybridization analysis of Lypd6 expression in the adult murine brain.

(B) Laminar expression of Lypd6 in the cortex. Staining was most prominent in layers IV, V and VI.

(C) Lypd6 positive staining in the vertical diagonal band of Broca (VDB).
(D) Lypd6 expression in paraventricular (PV), centrolateral (CL), intermediodorsal (IMD), paracentral (PC), central medial (CM) and reuniens (Re) thalamic nuclei.
(E) Lypd6 expression in dorsomedial hypothalamic nuclei (DM) and lateral hypothalamic area (LH). 3V = third ventricle. Bars represent (B) 200 μm and (C – E) 300 μm.

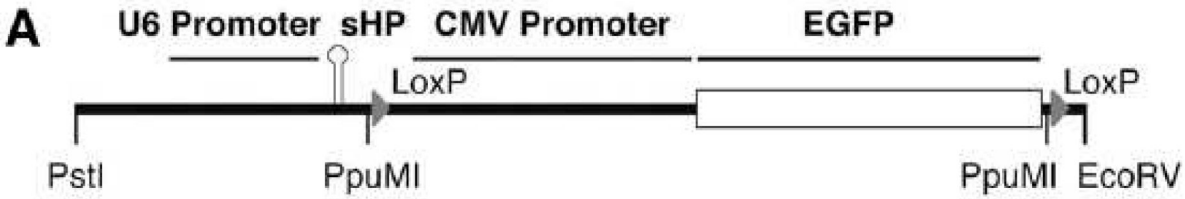

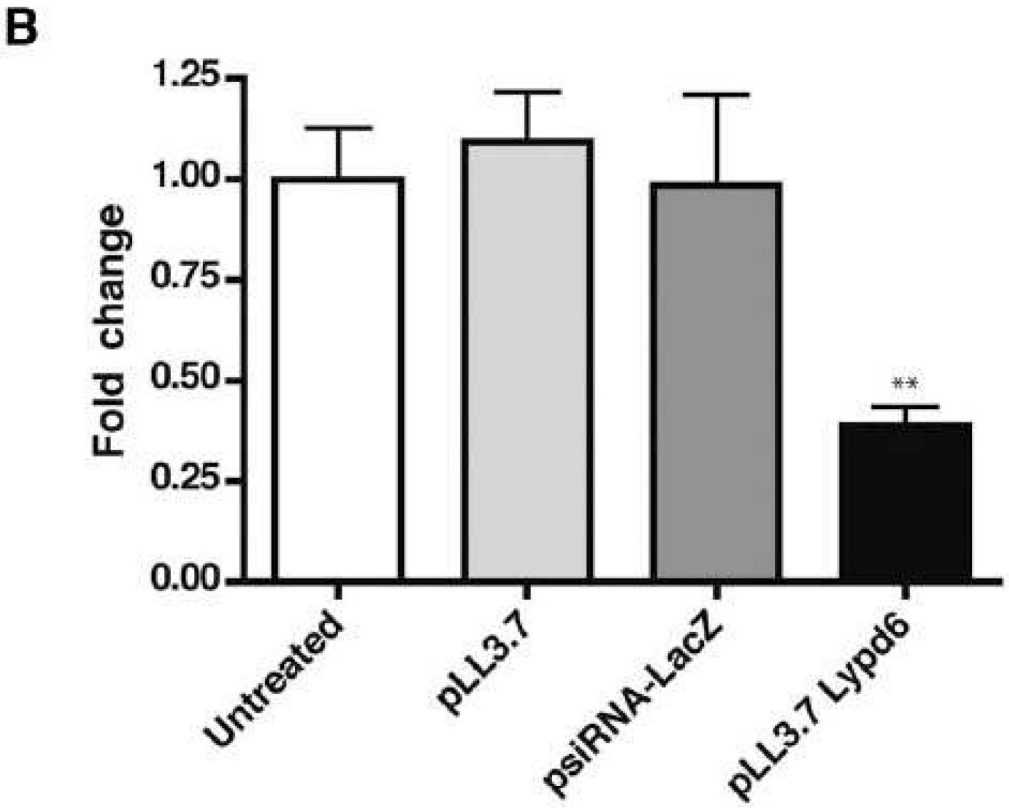

C

	m26	m21	m65	w54	w70	w82	Total
Wt	0	80	3	9	8	3	103
Tg	0	2	0	0	0	0	2
Total	0	82	3	9	8	3	105

Figure 3. Knockdown of Lypd6 transcription

(A) Knockdown construct (pLL3.7 Lypd6) used for ubiquitous silencing of Lypd6 expression. A small hairpin RNA (loop) was cloned behind the U6 promoter. A floxed (grey arrows) CMV promoter driven EGFP reporter gene (white box) was also included in the construct. Also shown are the restriction enzymes sites used for cloning and genotyping.

(B) Quantitative analysis of Lypd6 expression in Neuro-2a cells 36 h after transfection with pLL3.7 Lypd6 by RT-PCR. Expression was analyzed in untreated cells and cells transfected with empty vector (pLL3.7), off-target control (psiRNA-LacZ) or pLL3.7 Lypd6 plasmids. Lypd6 expression was normalized by TATA binding protein mRNA expression and then

calculated as fold change of untreated expression. **P < 0.05 for Dunnett's posttest between untreated and pLL3.7 Lypd6 transfected cells. Values are expressed as mean ± SEM.
(C) Total number of wild-type (Wt) and transgenic (Tg) offspring from three male (m26, m21 and m65), three female (w54, w70 and w82) transgenic founders and their transgenic offspring (m21_01 and m21_02).

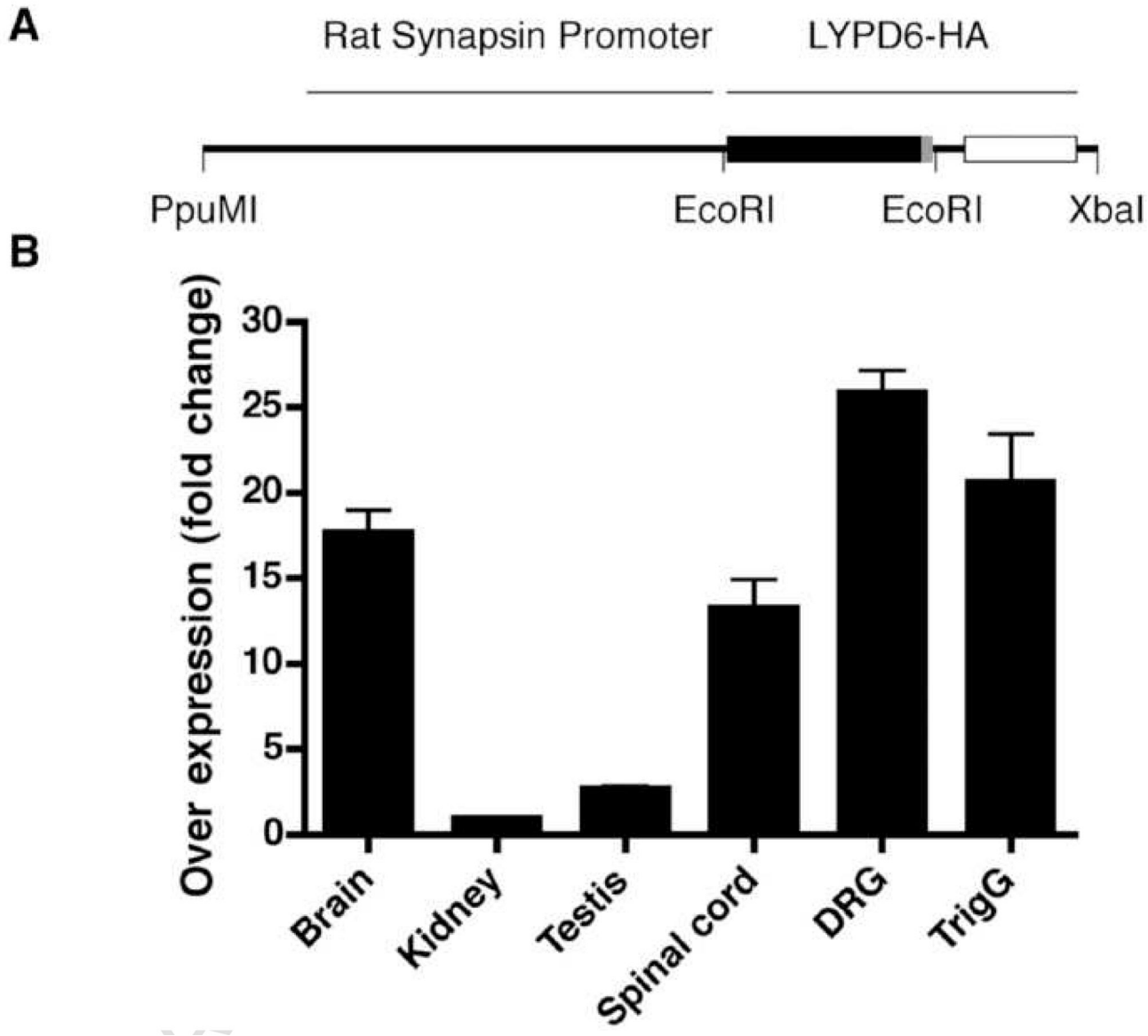

Figure 4. Lypd6 overexpression in the CNS of transgenic mice

(A) Expression construct for neuronal overexpression of Lypd6 in mice. The ORF of Lypd6 (black box) was fused to a haemagglutinin (HA) epitope (grey box) and cloned behind the rat Synapsin1 promoter. Shown in the white box is the bovine growth hormone polyadenylation signal. Restriction enzymes sites used for the cloning and genotyping are indicated.

(B) Quantitative analysis of Lypd6 overexpression in adult murine tissues of Synapsin-Lypd6 transgenic animals by real-time PCR. Lypd6 expression was first normalized to TATA binding protein mRNA expression and then calculated as fold change of wild-type expression. The analysis was performed independently with tissues from five animals. DRG = Dorsal root ganglia; TrigG = Trigeminal ganglia. Values on the y-axis are expressed as mean ± SEM.

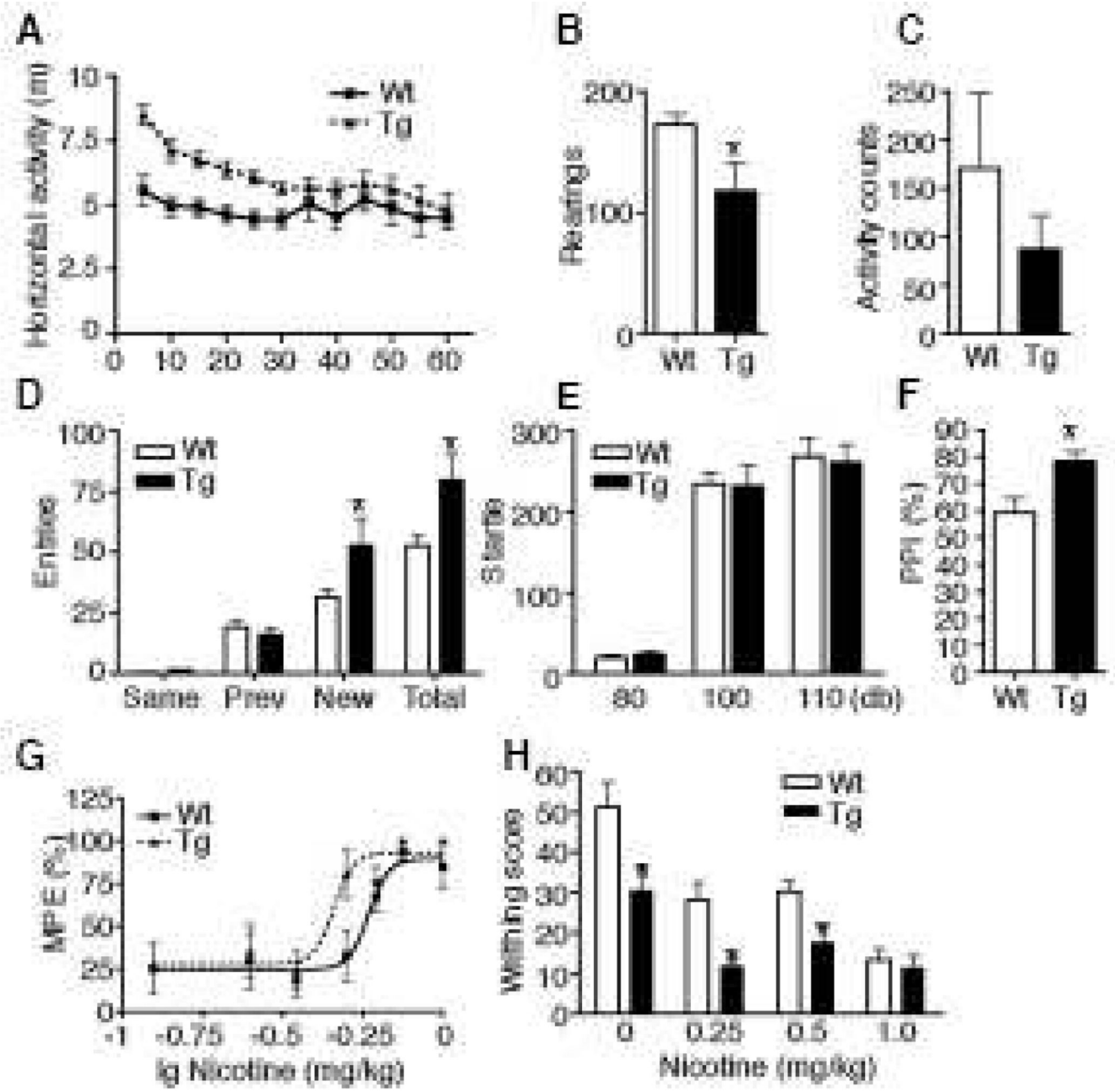

Figure 5. Behavioral effects of neuronal Lypd6 overexpression in transgenic mice

(A) Horizontal activity in the open field.

(B) Exploratory activity in the open field.

(C) Home cage activity.

(D) Entries to the same, previous or new arm and total number of entries in the Y-maze.

(E) Acoustic startle response.

(F) Prepulse inhibition of the acoustic startle response.

(G) Nociceptive responses in the tail-flick test after acute administration of saline or nicotine (0.125, 0.25, 0.35, 0.5, 0.625, 0.75 or 1 mg/kg s.c.). Nicotine dose effect: $P < 0.01$, $F_{6,98} = 14.13$, genotype effect: $P < 0.05$, $F_{1,98} = 4.13$; two-way ANOVA.

(H) Antinociceptive responses in the writhing test to acute co-administration of 0.6% acetic acid with saline or nicotine (0.25, 0.5, or 1 mg/kg s.c.). Nicotine dose effect: $P < 0.01$, $F_{3,72} = 19.33$, genotype effect: $P < 0.01$, $F_{1,72} = 17.42$; two-way ANOVA. Data represent means ± SEM for 8 to 10 mice per genotype and treatment. **P<0.01 and *P<0.05 for genotype comparisons with the Mann-Whitney test or Bonferroni post-hoc test. White bars indicate wild-type (Wt) and black bars transgenic (Tg) animals.

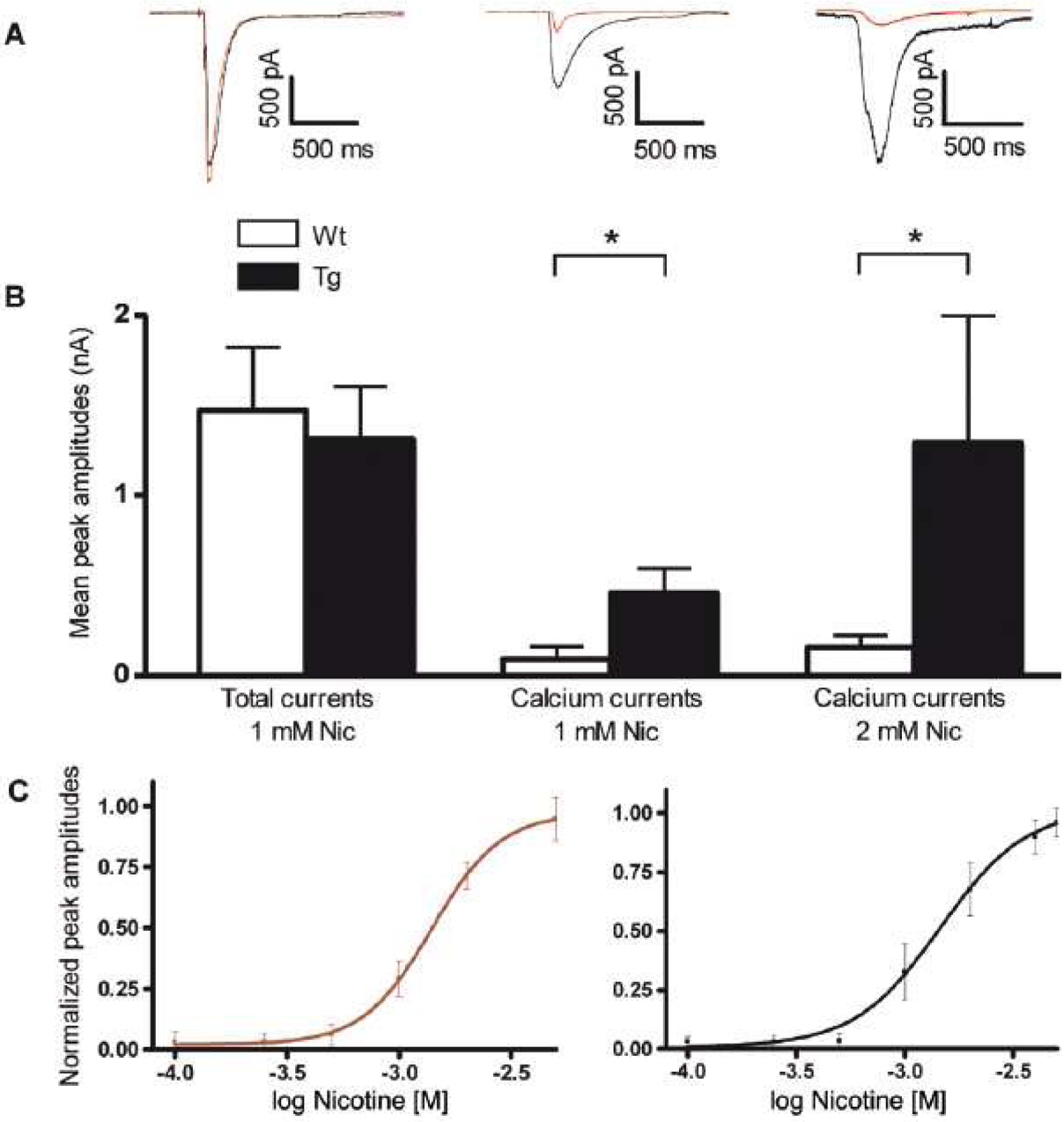

Figure 6. Ionic currents through nAChR-channels under different recording conditions in neurons of wild-type and transgenic animals

(A) Whole-cell current recordings from trigeminal ganglion neurons (TrigGs) elicited by nicotine in wild-type (red line) and Lypd6 transgenic (black line) mice (holding potential was −60 mV). Current traces in (A) compare to bar graphs below in (B). Currents through nAChR-channels were recorded with normal extra- and intracellular solution (Total currents) and with solutions isolating calcium current components (Calcium currents). Nicotine concentrations were as indicated.

(B) Bar graphs of mean peak amplitudes of total nicotine-evoked currents and calcium current components in wild-type (Wt) and transgenic (Tg) mice. Data represent means ± SEM for n = 5 (Wt) and n = 13 (Tg) for total currents; n = 11 (Wt) and n = 8 (Tg) for calcium currents 1

mM nicotine; n = 9 (Wt) and n = 5 (Tg) for calcium currents 2 mM nicotine. *P < 0.05 for the Mann-Whitney test.

(C) Dose-response curves for nicotine in TrigG neurons of wild-type (red) and transgenic (black) mice. Peak currents were normalized to maximum response. Each point represents mean ± SEM (n = 5 – 17). Wild-type: EC50 = 0.001396 M; Hillslope = 2.807 and transgenic: EC50 = 0.001456 M; Hillslope = 2.193.

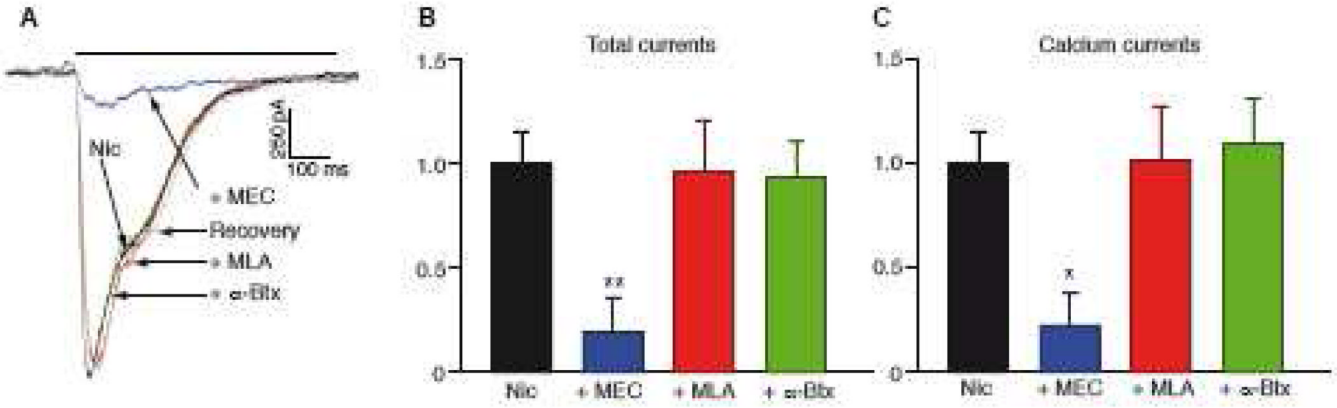

Figure 7. Pharmacology of currents through nAChR-channels

(A) Nicotine induced (3 mM) current responses recorded in the presence of mecamylamine (MEC, 20 μM), α-bungarotoxin (α-Btx, 100 nM) and methyllycaconitine (MLA, 20 nM) recorded in a single trigeminal ganglion neuron (black bar indicates application time). (B) Bar graphs showing total currents (Nic n = 20; MLA n = 8; α-Btx n = 9; MEC n = 14). (C) Bar graphs showing isolated calcium currents (Nic n = 19; MLA n = 16; α-Btx n = 18; MEC n = 6). *P < 0.05 and **P < 0.01 for the Mann-Whitney test.

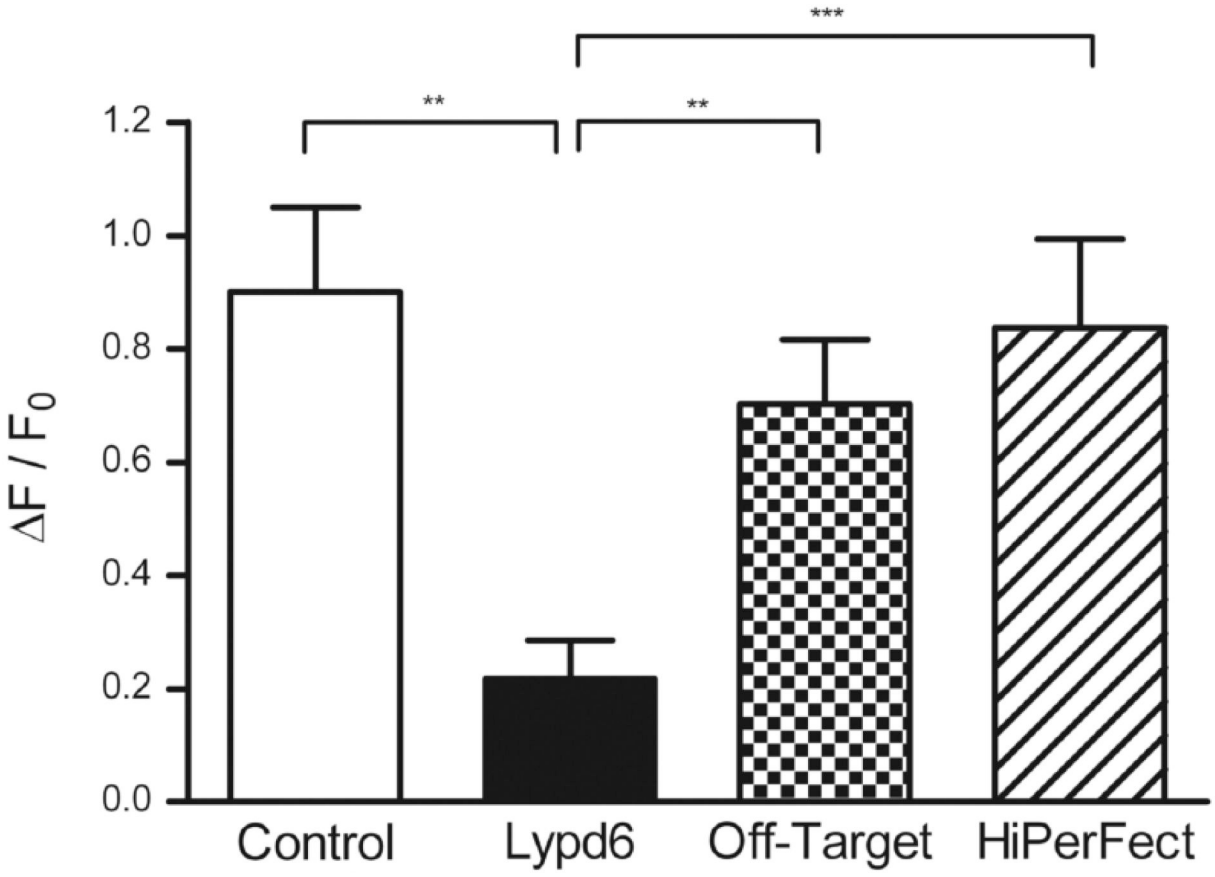

Figure 8. Microfluorometric measurements of intracellular calcium concentrations after siRNA treatment against Lypd6

Calcium transients evoked by nicotine application (3 mM) were measured in wild-type TrigG neurons after treatment with specific siRNA against Lypd6 (50 nM, black bar). The following controls were performed. White bar: Control without siRNA treatment, checker bar: Off-Target treatment with siRNA (50 nM) against Firefly Luciferase and dashed bar: HiPerFect treatment with HiPerFect transfection medium only. Each bar represents mean peak amplitudes of calcium transients ± SEM (n = 34 – 67). **P < 0.01 and ***P < 0.001 for the Mann-Whitney test.

Table 1

Breeding of pLL3.7 Lypd6 transgenic mice.

	m26	m21	m21_01	m21_02	m65	w54	w70	w82	Total
Wt	0	80	0	0	3	9	8	3	103
Tg	0	2	0	0	0	0	0	0	2
Total	0	82	0	0	3	9	8	3	105

Total number of wild-type (Wt) and transgenic (Tg) offspring from three male (m26, m21 and m65), three female (w54, w70 and w82) transgenic founders and their transgenic offspring (m21_01 and m21_02).